Electromagnetic decay of the 7.65-MeV state of $^{12}C^{\dagger}$

D. Chamberlin, D. Bodansky, W. W. Jacobs, and D. L. Oberg
Department of Physics, University of Washington, Seattle, Washington 98195
(Received 10 September 1973)

A measurement has been made of the branching ratio, Γ_{rad}/Γ, for electromagnetic transitions from the 7.65-MeV state of ^{12}C. This ratio is of particular interest in that the rate of ^{12}C synthesis in stellar helium burning is proportional to Γ_{rad}. The 7.65-MeV state was excited by inelastic scattering of 24-MeV α particles on ^{12}C, and electromagnetic transitions were identified by detecting coincidences between the inelastic α particles and the associated ^{12}C ions remaining after γ-ray or electron-pair emission. It was found that $\Gamma_{rad}/\Gamma = (4.2 \pm 0.2) \times 10^{-4}$, which may be compared to the previous best value of $(2.9 \pm 0.3) \times 10^{-4}$. The new result, combined with available information on the width and branching ratio for electron-pair emission, leads to a radiative width $\Gamma_{rad} = \Gamma_{\gamma} + \Gamma_{e^{\pm}} = (3.9 \pm 1.2)$ meV.

[NUCLEAR STRUCTURE ^{12}C, 7.65-MeV state; measured Γ_{rad}/Γ. Helium burning.]

I. INTRODUCTION

In the normal sequence of nucleosynthesis processes in stars the conversion of helium into heavier elements begins with the triple-α process, in which three α particles combine to form ^{12}C. The rate of this process is governed by the properties of the 0^+ second excited state of ^{12}C, which provides a fortuitously located resonance for the $^4He + {}^8Be \rightarrow {}^{12}C^*$ reaction at an excitation energy in ^{12}C of 7.65 MeV. For the most part, the 7.65-MeV state decays by α particle emission back to the ground state of ^8Be which quickly breaks up into two more α particles. However, there is a small branch for γ-ray emission to the bound state at 4.43 MeV and a much smaller branch for electron-pair emission directly to the ground state. The reaction rate for the triple-α process is proportional to the combined width, Γ_{rad}, for these electromagnetic transitions.[1]

To date, there has been no direct measurement of Γ_{rad}. Instead, Γ_{rad} has been determined from the relation[2]

$$\Gamma_{rad} = (\Gamma_{rad}/\Gamma)(\Gamma/\Gamma_{e^{\pm}})\Gamma_{e^{\pm}}$$

where the width, $\Gamma_{e^{\pm}}$, for electron-pair emission has been determined from inelastic electron scattering, and the branching ratios Γ_{rad}/Γ and $\Gamma_{e^{\pm}}/\Gamma$ have been directly measured.

A new measurement of Γ_{rad}/Γ is reported here. The 7.65-MeV state was excited through the inelastic scattering reaction $^{12}C(\alpha, \alpha')^{12}C^*$, and electromagnetic transitions were identified by detecting coincidences between α' and the ^{12}C ion remaining after γ decay or electron-pair emission. Aside from improvements in instrumentation, this approach is identical to that employed earlier by Eccles and Bodansky,[3] who found the branching ratio to be less than 0.001. Subsequent measurements have given an average value for the branching ratio of $\Gamma_{rad}/\Gamma = (2.9 \pm 0.3) \times 10^{-4}$. This average[2] is based on the work of Alburger,[4] who found $\Gamma_{rad}/\Gamma = (3.4 \pm 0.9) \times 10^{-4}$ in a study of p-γ-γ coincidences in the $^{10}B(^3He, p)^{12}C$ reaction (the number quoted here includes the small electron-pair emission branch), of Seeger and Kavanagh[5] who found $\Gamma_{rad}/\Gamma = (2.8 \pm 0.3) \times 10^{-4}$ in a study of α-^{12}C coincidences in the $^{14}N(d, \alpha)^{12}C$ reaction, and of Hall and Tanner[6] who found $\Gamma_{rad}/\Gamma = (3.5 \pm 1.2) \times 10^{-4}$ in a study of p-^{12}C coincidences in the $^{10}B(^3He, p)^{12}C$ reaction.

II. EXPERIMENTAL ARRANGEMENT

The experiment was performed with 24-MeV α particles from the University of Washington tandem Van de Graaff accelerator, with typical $^4He^{++}$ beam currents of about 0.5 μA. The physical arrangement is shown schematically in Fig. 1. Two versions of the arrangement, differing mainly in detector dimensions, were used, and are designated below as configurations A and B. Configuration A was used in all but the last group of runs.

In the coincidence technique used in the experiment it is important that the efficiency for interception of the ^{12}C ions be high. In principle, this could be achieved by using a large ^{12}C detector close to the target. Such a procedure would, however, increase the relative number of spurious events, increase dead-time losses, and make particle identification by time of flight more dif-

ficult. Therefore it is preferable to keep the spatial extent of the ^{12}C group small by having a small beam spot, a small α' detector solid angle, and as large a ^{12}C energy as possible (to minimize recoil effects accompanying γ-ray emission). These considerations, as well as those of counting rate and energy resolution, largely determined the choices made in the physical arrangement described in this section.

Preliminary to the coincidence measurement, the angular distribution for $^{12}C(\alpha, \alpha')^{12}C^*$ to the 7.65-MeV state was studied. With generally higher cross sections at forward angles and higher ^{12}C recoil energies at more backward angles, the most favorable α' angle was found to be at a secondary maximum near 65° (lab), where the differential cross section is approximately 4 mb/sr. Most of the experimental results were obtained at 65°; a smaller amount of data was taken at another maximum at 95°, where the cross section is about $\frac{1}{3}$ of the 65° cross section. The angles of the associated ^{12}C, for α' at 65 and 95°, are 37.6 and 25.0°, respectively.

The incident α-particle beam was focused by quadrupole magnets, and was further delimited by apertures in 0.8-mm-thick tantalum discs, placed in front of the target. For configuration A the smallest aperture was rectangular, 2.4 mm wide and 4.8 mm high, and for configuration B it was circular, 3.2 mm in diameter.

The carbon targets were self-supporting foils oriented so that the incident beam direction was normal to their plane. Target thicknesses were between 50 and 100 $\mu g/cm^2$, with the upper limit determined by the energy loss of the ^{12}C in the target. For these thicknesses multiple scattering represents only a small contribution to the overall angular divergence of the ^{12}C.

The α particles and the ^{12}C ions were detected

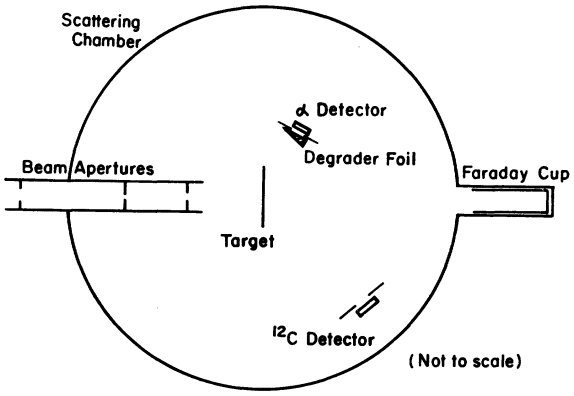

FIG. 1. Experimental arrangement (schematic).

in fully depleted surface-barrier solid-state detectors. The α' detector was 300 mm^2 in area and 200 μm thick, with a 0.95-cm diameter defining aperture at a distance of 20.3 cm from the target. For configuration A the ^{12}C detector was 100 mm^2 in area and 30 μm thick, with a 0.95-cm diameter aperture; for configuration B the detector was 300 mm^2 in area and 200 μm thick, with a 1.90-cm diameter aperture. In both cases data were taken with the ^{12}C detector at several distances from the target.

The relatively large angle subtended by the α' detector corresponds to a kinematic broadening across its face of 380 keV. An over-all resolution of 130 to 180 keV full width at half maximum (FWHM) for the 7.65-MeV peak was obtained by employment of a stepped degrader foil in front of the α' detector. The foil consisted of six successively thicker steps of gold evaporated on a nickel backing, with the thicknesses chosen so that α particles at different angles were degraded to the same final energy. The observed peak width with the foil is attributed largely to imperfections in the stepped degrader; the widths due to other effects, such as the finite beam spot size, the inherent detector resolution, or the energy loss in the target, were each not more than about 40 keV.

The spread in energy of the ^{12}C groups was determined mainly by target thickness. With the α' detector at 65° and the ^{12}C detector at 38° the recoil ^{12}C energy is 6.92 MeV, and the rate of energy loss[7] in the ^{12}C is 7.6 keV per $\mu g/cm^2$, corresponding to a total spread of about 700 keV for a typical target thickness of 75 $\mu g/cm^2$. γ-ray emission further changes the ^{12}C energy by up to 250 keV, the extreme case being when both γ rays are emitted in the original ^{12}C direction. Kinematic broadening, determined by the α' detector, had a full span of 380 keV. Contributions to the spread in pulse height from detector resolution effects were small in comparison.

The signals from each detector were processed through conventional fast and slow electronic systems. The fast system was used to select events with flight time differences characteristic of α'-^{12}C coincidences. In the final version, a signal from each detector was passed through a fast shaping amplifier to a high-low discriminator pair, where the low discriminator was used for leading-edge timing, and the high discriminator to establish an energy threshold. A fast coincidence between the discriminator outputs provided a relatively jitter-free timing pulse. The timing pulse from the α' detector was used as the start pulse for a time-to-amplitude converter, and the timing pulse from the ^{12}C system was used as the

stop pulse. The time resolution of the system for monoenergetic particles was about 0.8 nsec (FWHM), as measured at the shortest distances.

The slow electronic system provided pulses proportional to the particle energies in each detector. These two pulses, together with the output of the time-to-amplitude converter, were fed to an on-line XDS-930 computer. Each event was thus characterized by an α' energy ($E_{\alpha'}$), a recoil ^{12}C energy (E_R), and a time-of-flight difference (T). The computer was gated to accept only slow coincidence events for which $E_{\alpha'}$ and E_R exceeded appropriate thresholds, and T fell within the 100-nsec range of the time-to-amplitude converter.

Digitized signals for $E_{\alpha'}, E_R$, and T were written on magnetic tape for each accepted event. The computer provided oscilloscope displays and line printer outputs of the one-dimensional spectra for each of the three signals and of the two-dimensional spectra of E_R vs T and E_R vs $E_{\alpha'}$. The events included in either two-dimensional spectrum could be gated within the computer by windows imposed on the third signal; these windows could be repeatedly altered in off-line scans of the magnetic tape.

The computer system accepted only coincidence events. To provide data for determining the branching ratio, a singles spectrum from the α' detector alone was simultaneously collected in a one-dimensional multichannel analyzer. Dead time in the computer was kept low by the coincidence requirement; dead time in the multichannel analyzer was made small by gating the analyzer to accept only every tenth input pulse, with the attendant benefits of the scaler regularizing action.

A pulser system was used to monitor dead times and study suspected gain shifts. The pulser was triggered at a rate proportional to the beam current. The pulser signals were fed to the detector preamplifiers and were processed in a manner identical to that used for actual events, giving simulated coincident "$E_{\alpha'}$", "E_R", and "T" signals, as well as events to the multichannel analyzer. Comparison of the number of coincidence events and the number of multichannel analyzer events with the known number of pulser signals provided measures of the loss of counts, due to dead time or other causes, in both the coincidence system and in the multichannel analyzer system.

III. DATA COLLECTION AND ANALYSIS

Details of the geometric arrangements used for data collection are given in the first four columns of Table I. Under typical conditions, at 65° where most of the data were taken, the counting rate for coincidence events was about 40 events per hour. The ^{12}C solid angles covered in the two configurations, A and B, were the same, as both the distances and aperture diameters for the ^{12}C detector were twice as large for configuration B as for A.

The output format of the basic coincidence data of the experiment is illustrated in Fig. 2. In the lower spectrum the number of coincidence events is plotted as a function of α' energy, $E_{\alpha'}$, and ^{12}C energy, E_R. Events are included only if the time-of-flight difference T lies within the interval defined by the (adjustable) full time span of the upper spectrum. The strong group near $E_{\alpha'} = 10$ MeV

TABLE I. Determination of the branching ratio Γ_{rad}/Γ where θ = angle of α-particle detector (lab), L = distance of ^{12}C detector from the target, d = diameter of ^{12}C detector aperture, M = number of contributing runs, n_c = number of coincidence events, and ϵ = geometric efficiency. The third column specifies the use of configurations A or B.

θ (deg)	L (cm)	Conf.	d (cm)	M	n_c [a]	ϵ	Γ_{rad}/Γ [b] ($\times 10^4$)
65	15.2	A	0.95	4	397 ± 15	0.884 ± 0.022	4.34 ± 0.29
	20.3	A	0.95	6	894 ± 12	0.770 ± 0.035	4.27 ± 0.25
	25.4	A	0.95	3	394 ± 6	0.638 ± 0.031	3.87 ± 0.29
	30.5	B	1.90	2	532 ± 19	0.932 ± 0.020	4.07 ± 0.25
	40.6	B	1.90	3	503 ± 19	0.802 ± 0.021	4.25 ± 0.27
	50.8	B	1.90	1	353 ± 12	0.674 ± 0.021	4.30 ± 0.30
95	25.4	A	0.95	2	70 ± 3	0.774 ± 0.025	4.65 ± 0.59
	35.6	A	0.95	1	45 ± 2	0.581 ± 0.024	4.32 ± 0.69
						Weighted average [c]	4.20 ± 0.22

[a] The quoted uncertainties in n_c are the systematic uncertainties only.

[b] The quoted uncertainties in Γ_{rad}/Γ include both systematic and statistical standard deviations.

[c] The weighting is based on the uncertainties listed in column 8.

arises from α'-^{16}O coincidences from excitation of the 8.87-MeV state in ^{16}O. A 300-keV window around the 7.65-MeV group at $E_{\alpha'} = 9.4$ MeV is indicated by dotted lines and is used to gate the upper spectrum. The upper spectrum displays E_R vs T for the events falling within this window. The most prominent group is a band corresponding to the ^{12}C coincidences, with higher energy ^{12}C events (i.e., ^{12}C ions with less loss in the target or more energy from γ-ray recoil) appearing at smaller flight times. The total number of events in this band constitutes the number of coincidence events n_c used for determining the branching ratio. Values of n_c for the several experimental arrangements studied are listed in column 6 of Table I. In most cases the values are sums from several independent runs, as specified in column 5.

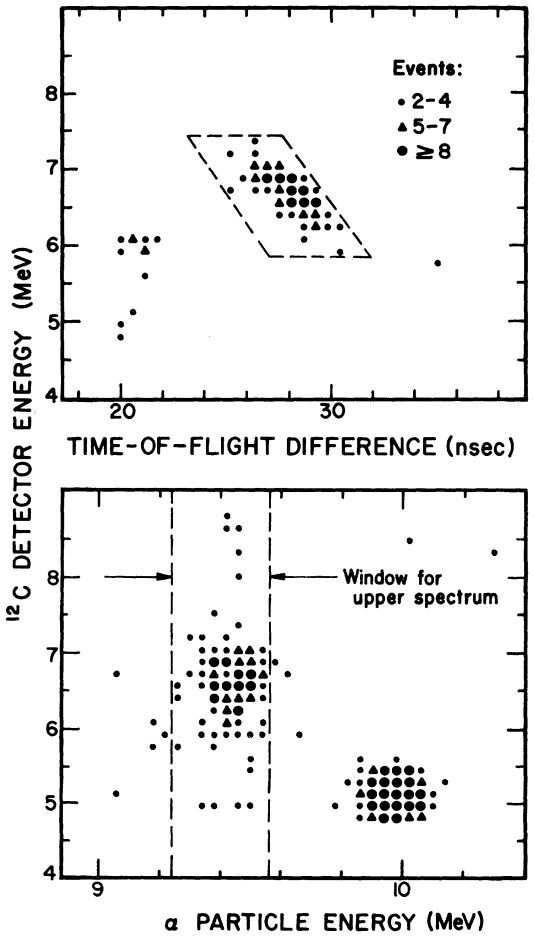

FIG. 2. Two-dimensional displays for coincidence data. For this run, configuration B was used with the ^{12}C detector at a distance of 40.6 cm from the target. The upper spectrum is gated by the 7.65-MeV α' group, as defined by the dotted lines in the lower spectrum.

A second particle group in the upper spectrum of Fig. 2, with shorter flight times, arises from the simultaneous detection in the ^{12}C detector of two of the α particles from the dominant decay mode of ^{12}C into ^{4}He + ^{8}Be. The time difference between this group and the ^{12}C group was sufficient for clear separation in all runs. Events in which all three α particles are detected are comparatively rare, and events in which only one α particle is detected give energies below the normal acceptance threshold in E_R.

The boundaries of the ^{12}C band, as well as of the α-particle window used for gating, are rather well defined, and could be checked by comparisons with spectra for other coincidence groups in the data, by comparisons with spectra obtained in the efficiency runs discussed below, and by examination of E_R vs T spectra for different $E_{\alpha'}$ windows. Nevertheless, there is some residual systematic uncertainty in assigning events to the group of interest. The estimated systematic uncertainties in n_c are tabulated together with n_c in column 6 of Table I. (Here, and elsewhere in quoting uncertainties, it is intended that the uncertainties be interpreted as roughly corresponding to standard deviations.) For the most part these uncertainties are less than 4%, but it is to be noted that these errors at different detector distances would tend to be positively correlated, and thus are not assumed to be reduced on combining the several data points.

The tabulated values of n_c include corrections for contributions from impurities in the target. In order to determine these corrections, data were taken with test targets rich in ^{13}C, ^{14}N, and ^{16}O, under conditions identical to those used in the normal data runs. Events closely simulating the events of interest can arise, for example, from inelastic scattering, followed by particle emission from the excited nucleus (n from ^{13}C, p from ^{14}N, or α from ^{16}O). The rate of these detected coincidence events should decrease roughly as the inverse square of the ^{12}C detector distance. By examining characteristic groups in the α-particle or two-dimensional spectra, the contaminant content of each target could be compared to that of the test targets. For the earliest data runs natural C targets were used, while for the bulk of the runs isotopically enriched ^{12}C was used, but even with the natural C targets the number of ^{13}C background events was less than 1% of the number of true events. With the α-particle detector at 65°, the contributions from ^{14}N and ^{16}O were also small for all targets. In aggregate at 65°, the total correction was found to be 3.3% with the ^{12}C detector at 15.2 cm from the target and less than 2% in the runs at greater distances. On the other

hand, with the α-particle detector at 95°, the measured corrections were 11.5% at 25.4 cm and 6.5% at 35.6 cm, arising primarily from ^{16}O. Uncertainties in these corrections are believed to be small compared to the corrections themselves.

As a further check on background events, test runs were taken in which the ^{12}C detector was displaced by 2.5 to 4.0° from its normal position. The observed rates for events within the ^{12}C band were very small, consistent with no events being seen from the 7.65-MeV state of ^{12}C, but with the contribution from the target impurities remaining. The persistence of impurity events was to be anticipated because the kinematic recoil cones, involving α-particle or nucleon emission following inelastic scattering, are large compared to the angular displacement of the detector in these runs.

The number of α particles N_S inelastically scattered from the 7.65-MeV state was determined from the multichannel analyzer spectrum illustrated in Fig. 3. The 7.65-MeV peak is well defined, with typical peak-to-valley ratios (for the low energy valley) in the neighborhood of 150 for the runs of configuration A and of 50 for the runs of configuration B. A background subtraction, based on the shape of the continuum, was made for each run; the resultant uncertainty in N_S was well under 1% and was taken to be negligible. The small errors introduced by the use of separate windows for defining N_S in the α' spectrum and for defining n_c in the two-dimensional spectrum are accounted for in the quoted systematic uncertainties for n_c in Table I.

The branching ratio for electromagnetic transitions is $\Gamma_{rad}/\Gamma = n_c/\epsilon N_S$, where ϵ is the geometric efficiency for the detection of ^{12}C and is defined by this relation. In determining the branching ratio an over-all correction was made for counting losses by comparing the total number of accepted events with the number of gating signals, for both the computer and the multichannel analyzer. Typically, these corrections were about 2% or less, although in some runs the corrections amounted to as much as 5%. Count losses inferred from the number of recorded pulser events confirmed these corrections, usually to within 1%. It was estimated that errors in this correction introduce an uncertainty of about 1% in the determination of the branching ratio.

The geometric efficiency ϵ for the 7.65-MeV state cannot be measured directly, but may be found by extrapolation from measured efficiencies for the ground state and 4.43-MeV state where $n_c/\epsilon N_S = 1$. Such measurements were made at angles where the ^{12}C has the same kinetic energy

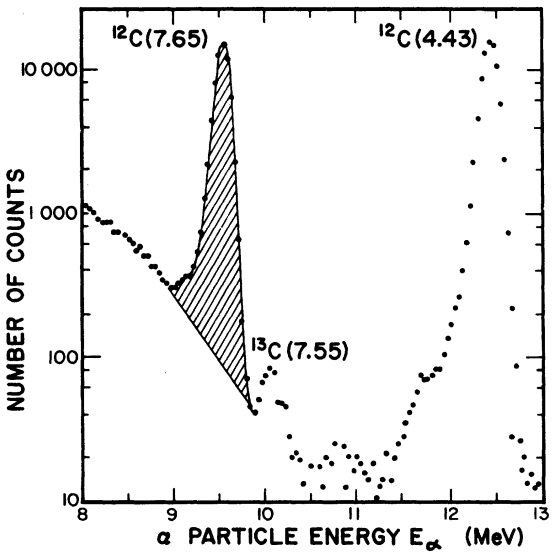

FIG. 3. Partial energy spectrum of scattered particles in the α' detector. The number of counts N_S in the 7.65-MeV peak is represented by the shaded area. (This spectrum is for the same run as displayed in Fig. 2 and has an unusually poor peak-to-valley ratio of 45.)

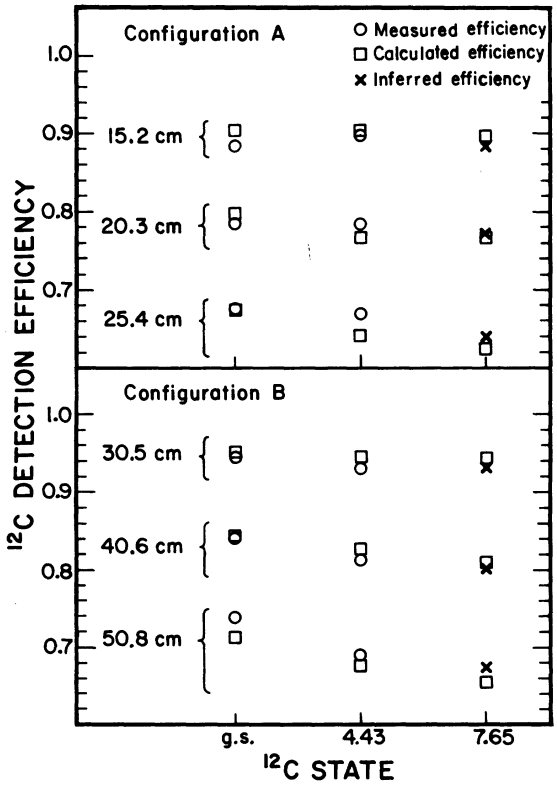

FIG. 4. Calculated and measured efficiencies for the detection of ^{12}C ions in coincidence with scattered α particles, together with the inferred efficiency for the 7.65-MeV state.

as for the case of the 7.65-MeV state. These measurements were interspersed among the regular data runs, and in addition to providing experimental determinations of ϵ, they were valuable for facilitating alignment and calibration of the system, for determining the energy and time resolution, and for verifying the stability and over-all performance of the system. Successive determinations of ϵ, for a given detector distance, were consistent within an rms deviation from their mean of about 3%. The average values of the measured geometric efficiencies are plotted in Fig. 4 for the several ^{12}C detector distances. As can be seen from the figure, in each configuration the measured efficiencies were near 90% at the smallest distances examined, and decreased with increasing distance.

The measured efficiencies are compared in Fig. 4 to efficiencies calculated from a Monte Carlo program, which traces the path of the ^{12}C after inelastic scattering. The program assigns values which define the location of the incident particle on the target, the direction of α', the direction of ^{12}C multiple scattering in the target, and the direction of emission of each γ ray. Each of the values was selected from an internally generated list of random numbers, with an appropriate weighting. In this weighting, the incident particles were assumed to be uniformly distributed over the beam spot, α' was assumed to be distributed uniformly over the α' detector, and the multiple scattering of the ^{12}C (taken to be fully ionized) was calculated using a standard simplified Gaussian form.[8] For the γ-ray cascade from the 0^+ 7.65-MeV state the actual angular distributions were used: the first γ ray is isotropic and the angular distribution of the second relative to the direction of the first is given by $W(\cos\theta) = \frac{5}{8}(1 - 3\cos^2\theta + 4\cos^4\theta)$. (The differences in recoil effects for the small electron pair branch are ignored.) For the decay of the 4.43-MeV state, an isotropic distribution was used in the absence of knowledge of the actual shape of the γ-ray distribution. However, trials with parameters representing extreme cases of the possible angular distributions[9] gave efficiencies differing by only about 2% from the efficiency for an isotropic distribution, at the largest ^{12}C detector distances.

The only free parameters in the Monte Carlo calculation were the assumed size of the beam spot on the target and, for configuration B, of a small offset of the beam center from its nominal position (motivated by evidence of such an offset in the appearance of the target after the runs). The effective beam spot depends upon how well the beam is focused. The fits to the measured ground-state and 4.43-MeV-state efficiencies were made by varying the beam spot diameter in the Monte Carlo calculation over the range from 80 to 100% of the smallest aperture diameter. Reasonable fits for configuration A were found for a beam spot 2.3 mm by 4.2 mm, and for configuration B for a beam spot 3.0 mm in diameter, offset from the nominal center by 1.1 mm. The corresponding efficiencies are displayed in Fig. 4 where for the ground state and 4.43-MeV state they can be compared to the measured efficiencies. The agreement is usually within 2%, and in the worst cases is within 4%. This relatively good agreement between the calculated and measured efficiencies confirms that the system was operating as expected, and lends confidence to the determination of the 7.65-MeV efficiency.

It is seen in Fig. 4 that the efficiencies, measured for the ground state and 4.43-MeV state and calculated for all three states, do not differ greatly from state to state. Because the efficiencies correspond to the same ^{12}C energies, multiple scattering in the target is the same in all three cases. The recoil due to γ-ray emission lowers the efficiency for the higher states, but this is balanced in part by the kinematic effects of their higher ratio of ^{12}C momentum to α' momentum. The inferred efficiencies for the 7.65-MeV state are essentially extrapolations of the measured efficiencies, guided by the excitation energy dependence of the calculated efficiencies. More explicitly, the inferred efficiency is equal to the

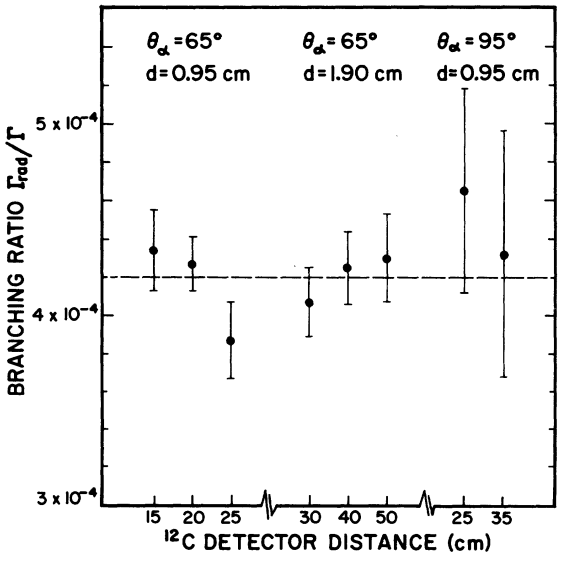

FIG. 5. Measured branching ratios, Γ_{rad}/Γ for two α' detector angles and several ^{12}C detector distances and aperture diameters. The indicated uncertainties are statistical standard deviations only. The dotted line is at the position of the weighted average $\Gamma_{rad}/\Gamma = 4.20 \times 10^{-4}$.

calculated efficiency for the 7.65-MeV state plus the mean difference between the measured and calculated efficiencies for the two other states.

These inferred efficiencies are plotted in Fig. 4 and are listed in column 7 of Table I. The indicated uncertainties in ϵ were calculated from a prescription based on an estimated over-all uncertainty in the measurements and calculation, together with additional uncertainties at each distance depending upon the consistency between the measured and calculated efficiencies and the magnitude of the difference between the calculated efficiencies for the 4.43- and 7.65-MeV states.

IV. RESULTS

The results for the several indicated geometries are summarized in column 8 of Table I and in Fig. 5. The quoted uncertainties in Table I include the statistical standard deviation in n_c, not listed elsewhere in the table, the systematic uncertainties in n_c and ϵ, as listed in columns 6 and 7, and the 1% uncertainty in the loss correction, cited above. Other uncertainties are believed to be small. The uncertainties plotted in Fig. 5 represent only the statistical standard deviations, and the results for the different distances and angles are seen to be consistent. The average value of the branching ratio from these measurements is

$$\Gamma_{rad}/\Gamma = (4.2 \pm 0.2) \times 10^{-4}.$$

The quoted uncertainty includes a 1.8% statistical contribution and an estimated over-all systematic uncertainty of 5% (the assigned systematic uncertainties for the individual 65° points range from 4.3 to 5.2%). This result is substantially larger than the previous best average, $\Gamma_{rad}/\Gamma = (2.9 \pm 0.3) \times 10^{-4}$. The branching ratio can be combined with results of measurements of the electron-pair-emission width[2] $\Gamma_{e^\pm} = (64 \pm 4)$ μeV and the electron-pair-branching ratio[10] $\Gamma_{e^\pm}/\Gamma = (6.9 \pm 2.1) \times 10^{-6}$, to determine the radiative width for the 7.65-MeV state to be $\Gamma_{rad} = (3.9 \pm 1.2)$ meV.

Quantitative treatment of stellar helium burning and of the resulting product abundances requires knowledge of the rates of both the triple-α process and the $^{12}C(\alpha,\gamma)^{16}O$ reaction.[11,12] The present results and recent measurements[13] establishing the excitation energy of the 7.65-MeV state to be (7.6542 ± 0.0016) MeV, place the determination of the triple-α rate on a more precise basis. Determination of the $^{12}C(\alpha,\gamma)^{16}O$ rate has presented formidable problems, but it is expected that studies now in progress[12] will substantially improve the situation. Pending the more complete calculations which the new nuclear information will make possible, we note that the higher value of Γ_{rad}/Γ found here corresponds to a 45% faster rate for the triple-α process at given temperature and density than follows from the earlier results for Γ_{rad}/Γ. Taken alone, this implies some increase in the ratio of the ^{12}C abundance to the ^{16}O abundance at the end of helium burning.

---

†Work supported in part by U. S. Atomic Energy Commission.

[1]See, e.g., E. M. Burbidge, G. R. Burbidge, W. A. Fowler, and F. Hoyle, Rev. Mod. Phys. 29, 547 (1957) for a discussion of the triple-α process.

[2]A summary of the measurements involved has been given by F. Ajzenberg-Selove and T. Lauritsen, Nucl. Phys. A114, 1 (1968).

[3]S. F. Eccles and D. Bodansky, Phys. Rev. 113, 608 (1959).

[4]D. E. Alburger, Phys. Rev. 124, 193 (1963).

[5]P. A. Seeger and R. W. Kavanagh, Nucl. Phys. 46, 577 (1963).

[6]I. Hall and N. W. Tanner, Nucl. Phys. 53, 673 (1963).

[7]L. C. Northcliffe and R. F. Schilling, Nucl. Data A7, 233 (1970).

[8]J. B. Marion and F. C. Young, *Nuclear Reaction Analysis* (North-Holland, Amsterdam, 1968), p. 30.

[9]T. D. Hayward and F. H. Schmidt, Phys. Rev. C 1, 923 (1970).

[10]D. E. Alburger, Phys. Rev. 118, 235 (1960); A. W. Obst, T. B. Grandy, and J. L. Weil, Phys. Rev. C 5, 738 (1972).

[11]R. J. Jaszczak, J. H. Gibbons, and R. L. Macklin, Phys. Rev. C 2, 63 (1970); R. J. Jaszczak and R. L. Macklin, *ibid.* 2, 2452 (1970).

[12]C. A. Barnes, P. Dyer, M. A. Dwarakanath, D. C. Weisser, and J. F. Morgan, Proceedings of the International Conference on Nuclear Physics, Munich, August, 1973, (to be published).

[13]S. M. Austin, G. F. Trentelman, and E. Kashy, Astrophys. J. 163, L79 (1971); H. Stocker, A. A. Rollefson, and C. P. Browne, Phys. Rev. C 4, 1028 (1971); S. J. McCaslin, F. M. Mann, and R. W. Kavanagh, Phys. Rev. C 7, 489 (1973).